

DOWNRANGE CONTROL GUIDANCE FOR REENTRY BURN OF REUSABLE LAUNCH VEHICLE

Ki-Wook Jung¹ & Chang-Hun Lee¹

¹Korean Advanced Institute of Science and Technology, Daejeon, 34141, Republic of Korea

Abstract

This research focuses on down-range correction during the reentry burn phase of Reusable Launch Vehicles (RLVs) to ensure a safe landing. Utilizing a partial-closed form solution for the aero-ballistic trajectory, we develop a guidance law in a feedback manner that controls the downrange distance during flight to a desired value during reentry. The partial-closed form solution is extended to the case with thrust, enabling accurate prediction of reentry trajectory. The proposed guidance law can ensure zero angle of attack at the end of the reentry burn, improving readiness for atmospheric entry. Additionally, it demonstrates sub-optimality in preserving the velocity reduction designated during the reentry burn. Validation through numerical simulations, based on initial conditions from commercial RLV missions, confirms the accurate performance and low computational load of the proposed method. This work can contribute to the development of efficient and effective guidance algorithms for RLVs, paving the way for more reliable RLV missions.

Keywords: Reusable Launch Vehicle, Reentry Burn, Zero-Effort-Miss, Finite-time Convergence

1. Introduction

The concept of a reusable launch vehicle (RLV) is beneficial to the operation of space flight missions both in terms of cost-effectiveness and flexibility. With the ongoing stable operation of RLVs demonstrated recently, the feasibility and practicality of RLVs are fairly established, which underscores the novel Guidance, Navigation, and Control (GNC) algorithms. The typical operation of RLV after the first-stage separation comprises kick-flip, reentry burn, aerodynamic descent, and landing burn with optional boost-back burn for further control over the trajectory. Current research in GNC algorithms predominantly focuses on the landing burn phase, accompanied by developments in computational guidance[1]. However, the trajectory deviation that can be endured by the landing burn is limited due to the brief duration of the landing burn and high dynamic pressure, even when maximized through numerical optimization. Therefore, it is crucial for the onboard guidance system of the RLV to effectively regulate trajectory deviations during earlier phases, such as the reentry burn and aerodynamic descent, to steer the vehicle accurately towards the landing site. Given the lack of control over the trajectory for a significant duration before reentry burn, the ability to correct trajectory deviations during this phase is vital for the robust operation of RLVs.

There are few previous works that utilize thrust acceleration to correct the trajectory deviation or instantaneous impact point (IIP), which is defined as the impact point of the vehicle assuming there is no further thrust force. The ability to accurately predict the impact point may generate efficient guidance laws that control an impact point. In this context, the analytical expression of the IIP, based on Keplerian orbit equations, has been derived[2] and employed to design guidance laws[3, 4] that can steer the IIP towards a desired location. However, due to the exclusion of the aerodynamics, primarily the quadratic drag, the IIP may have position error in order of several kilometers after the reentry of RLV to the atmosphere. Furthermore, trajectory deviation by the remaining duration of thrust is not considered, which can induce unnecessary maneuvers. Obtaining an analytical solution for an aeroballistic trajectory is practically infeasible, even when assuming a planar Earth, thus necessitating

a numerical approach. In other works, the aero-ballistic trajectory of flight vehicle is predicted[5, 6] through numerical integration. To reduce the computational load, a partial-closed form solution[7] for the motion of the mass in the quadratic drag with constant gravity is utilized. This accurate prediction of aero-ballistic enables the resulting guidance law to have desirable properties such as reduced control effort and zero guidance command at the terminal phase. However, as these methods do not account for thrust during descent, they are not directly applicable for guidance during the reentry burn.

Based on these observations, this research focuses on the downrange distance correction during the RLV's reentry burn. We propose a guidance law that controls the downrange distance to the desired value in a feedback form. Similar to previous work [6], a partial-closed form solution of the aero-ballistic trajectory is used to accurately predict the descent trajectory of the RLV. The extension of the partial-closed form solution is found to naturally augment the reentry burn phase to the trajectory prediction. Based on this extended trajectory prediction, the proposed guidance law can have reduced correcting maneuver and zero angle of attack (AoA) at the end of the reentry burn, which can improve readiness prior to entering the atmosphere. Moreover, it is found that the devised guidance law has sub-optimality in terms of preserving the designated ΔV for the reentry burn. The performance and characteristics of this guidance law are validated through numerical simulations using initial conditions based on commercially operational RLV missions, demonstrating both the effectiveness and low computational load of the proposed method.

This paper is organized in the following manner. In Section 2. the vehicle dynamics and rapid prediction method for reentry trajectory are presented. Section 3. provides a detailed description and analysis of the proposed guidance law. Numerical results are provided and discussed in Section 4., followed by the concluding remarks in Section 5.

2. Problem Formulation

In this section, the guidance problem handled in this work is established and the rapid trajectory prediction method utilized in this work is described.

2.1 Vehicle Dynamics

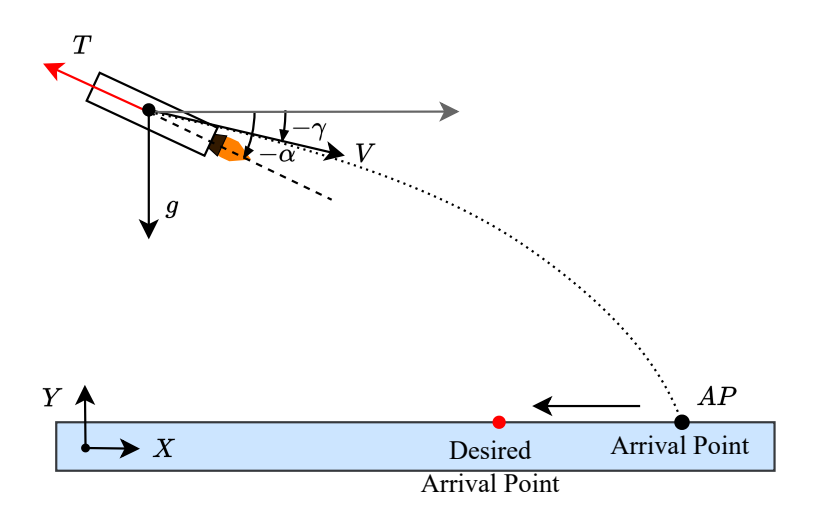


Figure 1 – Vehicle Kinematics

This section describes the dynamics model of the reusable launch vehicle (RLV) considered in this work. Based on the observation that the typical vertical take-off vertical landing (VTVL) type RLV experiences a relatively steep flight path angle during reentry and following aerodynamic descent with minimal lift force, we ignore the curvature of the earth surface and derive the dynamics assuming the 2D planar motion of the RLV as depicted in Fig. 1. (X,Y) are the axes of the inertial reference frame (I-frame), and Y is in upward direction, perpendicular to the earth surface. The vehicle dynamics is

given as

$$\dot{x} = V \sin \gamma
\dot{y} = V \cos \gamma
\dot{V} = a_V - g(y) \sin \gamma
\dot{\gamma} = -\frac{g(y) \cos \gamma}{V} + \frac{a_{\gamma}}{V}$$
(1)

In Equation (1), V is the magnitude of the velocity and γ is the flight path angle as described in Fig. 1. The acceleration due to the external forces a_V and a_γ are defined as follows:

$$a_V = \frac{1}{m} \left(-\bar{q} S_{ref} C_D - T \cos \alpha \right) \tag{2}$$

$$a_{\gamma} = \frac{1}{m} \left(\bar{q} S_{ref} C_L - T \sin \alpha \right) \tag{3}$$

 S_{ref} is the reference area of the vehicle and \bar{q} is the dynamic pressure computed defined as $\frac{1}{2}\rho V^2$. The thrust force T is a function of time since the rocket engine is only active during the reentry burn. The gravitational attraction is assumed to have only vertical component and is modeled as the function of altitude.

$$g(y) = g_{ref} \frac{(y + r_{ref})^2}{r_{ref}^2}$$
 (4)

In Equation 4, g_{ref} is the reference value of the gravitational acceleration, and r_{ref} is the reference radius that defines g_{ref} .

2.2 Rapid Prediction

The proposed guidance law in this work is based on the accurate prediction of the descent trajectory that includes reentry burn and aerodynamic descent. The descent trajectory depends on the angle of attack, α . In this work, we define the zero-effort trajectory as the trajectory that results from the zero α throughout the descent and predict the zero-effort descent trajectory. The main concept behind defining the zero-effort trajectory is to ensure that no additional maneuvers, other than a gravity turn, are required for the RLV after the termination of the guidance.

To predict the zero-effort descent trajectory with the presence of quadratic drag and no thrust force, numerical integration of the dynamics in Eq. (1) can give accurate trajectory prediction. However, to improve the computational efficiency without loss of accuracy, which can improve the feasibility and practicability of the proposed method for onboard implementation, we employ a partial-closed form solution of the aero-ballistic trajectory. Assuming constant ballistic coefficient β and g for short duration of trajectory, an analytical relationship between V and γ can be derived.

$$V(\gamma) = \frac{V_0 \cos \gamma}{\cos \gamma \sqrt{1 + \beta V_0^2 \cos^2 \gamma_0 (f(\gamma_0) - f(\gamma))}},$$
where $\beta \triangleq \frac{\rho C_D S_{ref}}{mg}, \ f(\gamma) \triangleq \frac{\sin \gamma}{\cos^2 \gamma} + \ln \left[\left(\frac{\gamma}{2} + \frac{\pi}{4} \right) \right]$ (5)

The subscript "0" in Eq. (5) denotes the initial value of each state variable. Based on Eq. (5), the partial-closed form solution in form of integration with γ as an independent variable was derived in the previous work[7] as follows.

$$t_{k+1} = t_k + \frac{2\left[V_k \sin \gamma_k - V_{k+1} \sin \gamma_{k+1}\right]}{g_k \left(2 + \mu_k^A\right)},$$

$$x_{k+1} = x_k + \frac{V_k^2 \sin 2\gamma_k - V_{k+1}^2 \sin 2\gamma_{k+1}}{2g_k \left(1 + \mu_k^A\right)},$$

$$y_{k+1} = y_k + \frac{V_k^2 \sin^2 \gamma_k - V_{k+1}^2 \sin^2 \gamma_{k+1}}{g_k \left(2 + \mu_k^A\right)},$$
where $\mu_k^A = \beta_k \left(V_k^2 \sin \gamma_k + V_{k+1}^2 \sin \gamma_{k+1}\right)$

Since the integration formula in Eq. (6) leverages several analytical relations between state variables, the integration step $\Delta \gamma$ can relatively be large without sacrificing prediction accuracy, which accomplishes rapid prediction of trajectory. In this work, the computational efficiency of Eq. (6) relative to the Euler integration of Eq. (1) was approximately three-fold, measured by the CPU time needed to reach the same level of accuracy.

However, in the prediction of complete descent from reentry burn to the touch down to the earth's surface, the thrust force should be considered during reentry burn. The reentry burn usually occurs before the vehicle reaches the significant dynamic pressure to reduce the aerodynamic load and heat flux of the RLVs. Therefore, aerodynamic forces can be ignored during the reentry burn due to the negligible dynamic pressure. In this work, we derive another partial-closed form solution for the case with constant thrust acceleration without drag. The velocity dynamics can be rewritten as,

$$\dot{V} = -g\sin\gamma - gK_T$$
, where $K_T \triangleq \frac{T}{mg}$ (7)

It is important to note that the vehicle mass m changes as the propellant is depleted during engine ignition, which makes K_T a time-varying variable, not a constant. This disparity in dynamics is later compensated by a non-iterative corrector. The analytical relationship between V and γ assuming constant K_T can be found as follows

$$V(\gamma) = \frac{V_0 F(\gamma)}{F(\gamma_0)}, \text{ where } F(\gamma) \triangleq \frac{\left(\cos\frac{\gamma}{2} - \sin\frac{\gamma}{2}\right)^{-K_T} \left(\cos\frac{\gamma}{2} + \sin\frac{\gamma}{2}\right)^{-K_T}}{\cos\gamma} \tag{8}$$

Then, after a process of derivation of partial-closed form similar to [7], it is found out that identical formula in Eq. (6) can be used with only μ_k^A being replaced by μ_k^T defined as below

$$\mu_k^T = K_T \left(\sin \gamma_k + \sin \gamma_{k+1} \right) \tag{9}$$

Lastly, to compensate for the time-varying m, the integration is repeated with $m'_k = m_k - \dot{m}(t_{k+1} - t_k)$ after initial integration with m_k for each integration step k. Then, the state variables of next step k+1 are decided as the average value of first and second iteration.

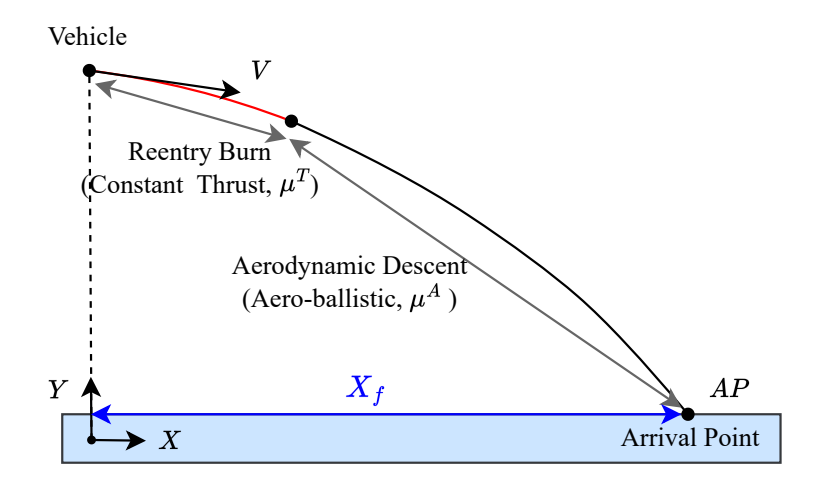


Figure 2 – Trajectory prediction by partial-closed form solution

As a result, we can predict the complete zero-effort descent trajectory through two separate partial-closed form solutions as in Fig. 2. Since the duration of reentry burn is usually pre-programmed to obtain enough kinetic energy reduction, the reentry burn phase is predicted by Eqs. (6) and (9) from current states with prescribed duration of time. Aerodynamic descent trajectory is predicted by Eq. (6) from final states of reentry burn till touchdown to the prescribed terminal altitude, usually the earth's surface. Hereafter, the downrange distance during the descent trajectory, X_f in Fig. 2, is expressed as the function of a certain set of parameters Θ , which consists of current states of the vehicle and remaining duration of the reentry burn, t_b .

$$X_f = f_r(\Theta), \text{ where } \Theta \triangleq [y, V, \gamma, m, t_b]^T$$
 (10)

3. Proposed Method

In this section, the proposed algorithm is described in detail from the guidance objective to the analysis on the guidance law characteristics.

3.1 Guidance Objective

In this work, the downrange distance achieved by the RLV is controlled to steer the RLV to the desired arrival point (AP) such as the landing site or safety zone for ground impact. We define x_d as the desired downrange position of the AP for the RLV. Then, the zero-effort-miss (ZEM), Z is defined as follows.

$$Z(t) = [x_d - x(t)] - f_r(\Theta(t))$$
(11)

The proposed guidance law aims to nullify ZEM during the duration of the reentry burn.

3.2 Guidance Derivation

3.2.1 Dynamics of ZEM

Z(t) is the constant throughout the flight assuming that trajectory prediction is completely accurate, as long as the AoA is zero. To obtain the control authority over the ZEM, we compute the Z's time derivative.

$$\frac{dZ}{dt} = -V\sin\gamma - \frac{df_r(\Theta)}{dt} - \Delta \left[\frac{df_r}{dt} \right] = -\Delta \left[\frac{df_r(\Theta)}{dt} \right]. \tag{12}$$

In Equation (12), $\frac{df_r(\Theta)}{dt}$ is the time-derivative of X_f with zero AoA and identical to the $-\dot{x}$. $\Delta\left[\frac{df_r(\Theta)}{dt}\right]$ is the perturbation in time-derivative of X_f when non-zero AoA exists. The $\Delta\left[\frac{df_r(\Theta)}{dt}\right]$ can be expanded in following form using chain-rule for Θ .

$$\Delta \left[\frac{df_r(\Theta)}{dt} \right] = \frac{\partial f_r}{\partial V} \Delta \dot{V} + \frac{\partial f_r}{\partial \gamma} \Delta \dot{\gamma} = \frac{\partial f_r}{\partial V} \left(\frac{-T(1 - \cos \alpha)}{m} \right) + \frac{\partial f_r}{\partial \gamma} \left(\frac{-T \sin \alpha}{mV} \right) \\
\approx \frac{\partial f_r}{\partial \gamma} \left(\frac{-T \sin \alpha}{mV} \right) = F_{\gamma} \sin \alpha \tag{13}$$

Since the effect of aerodynamic forces is negligible during reentry burn, aerodynamic forces are omitted in Eq. (13). Also, assuming that the amount of downrange correction is not large enough to generate substantial AoA, the term $(1-\cos\alpha)$ is approximated to 0. Equation (13) implies that the appropriate generation of AoA can steer the RLV to the desired AP by controlling the time derivative of Z.

3.2.2 Guidance Command

The guidance problem handled in this work is the finite-time convergence problem since the guidance objective Z should be nullified before the termination of the reentry burn. It is worth noting that the remaining trajectory deviation can further be corrected throughout the aerodynamic descent by the guidance algorithms in [6, 8]. However, the control authority of thrust over the trajectory is significantly higher than that of aerodynamic forces, emphasizing the importance of nullifying ZEM during the reentry burn. Therefore, we employ the finite-time convergent error dynamics in related work[9] for the derivation of guidance command.

$$\dot{Z} + \frac{KZ}{t_{go}} = 0$$
, where $K \in \mathbb{R}^{++}$. (14)

K in Eq. (14) is positive scalar and serves as guidance gain. If the desired dynamics in Eq. (14) are achieved, the Z converges in the following pattern.

$$Z(t) = Z(t_0) \left(\frac{t_b}{t_{b,0}}\right)^K \tag{15}$$

Here, $t_{b,0}$ is the total duration of the reentry burn. From Equation (15), it is evident that a positive guidance gain K ensures convergence of Z to zero as $t_b \to 0$.

We can derive the guidance command by utilizing feedback linearization to accomplish the desired dynamics in Eq. (14). Since the time-derivative of Z depends on the AoA as in Eq. (13), the guidance command is given as AoA command during reentry burn.

$$\dot{Z} + \frac{KZ}{t_b} = F_{\gamma} \sin \alpha + \frac{KZ}{t_b} = 0, \quad \therefore \alpha_c = \sin^{-1} \left(-\frac{KZ}{F_{\gamma} t_b} \right)$$
 (16)

The sensitivity coefficient $\frac{\partial f_r}{\partial \gamma}$ can be numerically computed by an additional trajectory prediction with slight perturbation in initial γ .

$$\frac{\partial f_r}{\partial \gamma} \approx \frac{f_r(\Theta') - f_r(\Theta)}{\Delta \gamma}, \text{ where } \Theta' = [y, V, \gamma + \Delta \gamma, m, t_b]^T$$
 (17)

3.3 Guidance Characteristics

In this section, the analysis of the optimality and property of the proposed guidance is provided.

3.3.1 Optimality Analysis

For analysis, we approximate the guidance command in Eq. (16) as follows based on small angle approximation.

$$\alpha_c = \sin\left(-\frac{KZ}{F_{\gamma}t_b}\right) \approx -\frac{KZ}{F_{\gamma}t_b}$$
 (18)

According to previous work [9], the cost function minimized by the guidance command in Eq. (18) is found as follows.

min
$$J = \int_{t_0}^{t_f} \frac{1}{t_{go}^{K-1}} F_{\gamma}^2 \alpha^2 dt = \int_{t_0}^{t_f} \frac{1}{t_{go}^{K-1}} \left(\frac{\partial f_r}{\partial \gamma}^2 \frac{T}{mV^2} \right) \frac{T}{m} \alpha^2 dt$$

$$= \int_{t_0}^{t_f} W(t) \frac{T}{2m} \alpha^2 dt, \text{ where } t_f = t_0 + t_{b,0}$$
(19)

From Equation (19), the cost function J has a form of minimizing the integral of the weighted quadratic function of α .

The main purpose of the reentry burn is deceleration by the retro-propulsion prior to the atmospheric entry. In the stage of trajectory design, the ΔV to be decreased during reentry burn is usually decided assuming no AoA. This prescribed ΔV should be kept as much as possible even with the deployment of closed-loop guidance. In this perspective, the physical meaning of Eq. (19) can be found from the velocity dynamics in Eq. (1). The change in velocity dynamics from no AoA to the non-zero AoA can be expressed in the following form.

$$\Delta \dot{V} = \dot{V} - \dot{V}_{\alpha=0} = \frac{T}{m} (1 - \cos \alpha) \approx \frac{T}{2m} \alpha^2$$
 (20)

Then, total change in velocity decrease due to the AoA during reentry burn is

$$\Delta V_{\mathsf{loss}} = \int_{t_0}^{t_f} \Delta \dot{V} dt \approx \int_{t_0}^{t_f} \frac{T}{2m} \alpha^2 dt \tag{21}$$

By comparing the Eq. (19) and Eq. (21), we can observe that the cost function of the proposed guidance algorithm can be interpreted as the minimization of $\Delta V_{\rm loss}$ with a weighting function W(t). Due to the approximations during the derivation of Eq. (19) and the existence of W(t), the difference between Eq. (19) and $\Delta V_{\rm loss}$ may vary. However, we can still conclude that the proposed guidance can regulate the amount of the $\Delta V_{\rm loss}$.

3.3.2 Guidance Gain Selection

It is beneficial for the guidance law to result in zero AoA at the terminal phase for the transition to atmospheric entry. For the analysis conducted in this section, the rotational or actuator dynamics are

assumed to be fast enough to be ignored. In the ideal case where the dynamics in Eq. (14) is exactly accomplished, the guidance command can be expressed as follows combining Eqs. (15) and (22).

$$\alpha_c = \frac{KZ_0}{F_{\gamma}t_{b,0}} \left(\frac{t_b}{t_{b,0}}\right)^{K-1}$$
 (22)

Thus, K larger than 1 can result in zero AoA command as $t_b \to 0$. However, there may exist disturbances and omitted dynamics in Eq. (14), which makes k > 1 just a necessary condition. Therefore, we consider dynamics with uncertainties represented as d.

$$\dot{Z}=F_{\gamma}'\alpha+d(Z), \text{ where } d(Z)=a_1Z+a_2Z^2$$

$$F_{\gamma}',a_i\in\mathbb{R},\quad i=1,2$$
 (23)

The uncertain control effectiveness F'_{γ} is assumed to have same sign as F_{γ} and non-zero. a_1 approximately represents dynamics error proportional to ZEM, while a_2 mainly represents the potentially omitted higher-order dynamics. Also, the magnitudes of the coefficients F'_{γ} and a_i are assumed to be bounded, since the dynamics error or disturbances should be finite in the real-world scenario.

$$|F'_{\gamma}| \ge \underline{F}_{\gamma}, \quad |a_i| \le \bar{a}_i, \quad i = 1, 2$$
 (24)

Then, we propose following Lemma to find a sufficient condition for the $\alpha_c(t_b=0)=0$.

Lemma 1 If K' > 1 exists such that $\dot{Z} \leq -\frac{K'}{t_b}Z$ for $t \in [t_0, t_f]$, α converges to 0 at $t_b = 0$.

For the proof of Lemma 1, first we assume $Z_0 > 0$ without loss of generality. When the condition regarding K' in Lemma 1 is satisfied, the following upper bound can be found for the Z(t).

$$Z(t) \le Z_0 \left(\frac{t_b}{t_{b,0}}\right)^{K'}, \ \forall t \in [t_0, t_f]$$
 (25)

From Eq. (22), we can observe that α becomes 0 at $t = t_f$ when Z is bounded as in Eq. (25), which completes the proof. Utilizing Lemma 1, we seek the existence of K' for uncertain dynamics in Eq. (23).

$$\dot{Z} = -(\eta K - a_1 t_b - a_2 Z t_b) \frac{Z}{t_b}$$
, where $\eta \triangleq \frac{F'_{\gamma}}{F_{\gamma}} > 0$ (26)

The lower bound of the coefficient for $-Z/t_b$ in RHS of Eq. (26) can be found as follows

$$\eta K - a_1 t_b - a_2 Z t_b \ge \underline{\eta} K - \bar{a}_1 t_{b,0} - \bar{a}_2 t_{b,0} Z,$$

$$\underline{\eta} = \min \eta = \frac{F_{\gamma}}{F_{\gamma}}$$
(27)

In Equation (27), if we select the guidance gain that satisfies the Condition 1 in Eq. (28) at initial time, the time derivative of Z becomes negative for $t \in [t_0, t_f]$ and the upper bound can be found as follows.

This implies setting the large enough K can guarantee the existence of the K' in Lemma 1.

$$K + a_1 t_h + a_2 Z t_h > K' > 1$$
 (29)

Therefore, Condition 1 is the sufficient condition for $\alpha_c(t_b=0)=0$. It is worth noting that finding the exact values of $\underline{\eta}$, \bar{a}_1 and \bar{a}_2 might not be straightforward. Nevertheless, the analysis result in this work indicates that an appropriately selected gain K can converge α to 0.

4. Numerical Results

In this section, the numerical simulation results are provided to verify the performance and characteristics of the proposed guidance law. The RLV specifications and trajectory parameters are approximately attained from one of the LEO missions of SpaceX's Falcon 9 rocket. The initial conditions and vehicle parameters used in this work are presented in Table. 1. Also, the aerodynamics data are attained from the related work[10], where the detailed aerodynamic coefficients are provided for the reentering rocket booster. Initial downrange position *x* is set to give the desired initial ZEM.

Table 1 – Simulation parameters

Parameter	Value	Parameter	Value
$\overline{m_0}$	47.466 Ton	У0	66.742 km
S_{ref}	$10.75 \ m^2$	γ_0	-25.14 deg
$T^{'}$	247.5 kN	V_0	2211 m/s
I_{sp}	282 sec	$\Delta \gamma$	-0.2 deg
$t_{b,0}$	20 sec		

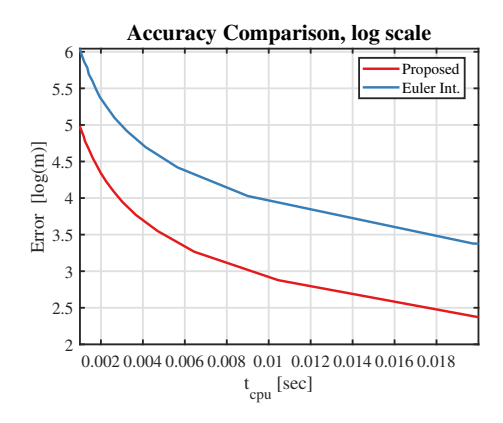


Figure 3 – Accuracy comparison

First, Figure 3 shows the numerical efficiency comparison between the proposed rapid prediction and Euler integration of (1) with initial conditions in Table. 1. The rapid prediction method used in this work shows 3 times faster prediction speed for same accuracy level achieved by Euler integration. This demonstrates the proposed prediction method can increase the applicability of the proposed guidance law.

4.1 Case Study - ZEM

Numerical simulation is conducted with initial conditions in Table. 1 by varying the initial ZEM from -10 km to 10 km with 5 km interval to review the guidance performance under various initial condition. The guidance gain K is set to 1, and the results are presented in Fig. 4.

For all initial ZEMs, the proposed guidance law successfully nullified the ZEM within the duration of the reentry burn. The ZEM profile in Fig. 4b shows that desired error dynamics are well accomplished by displaying a pattern of $Z(t) = Z_0 \frac{t_b}{t_{b,0}}$. Accordingly, the angle of attack history of each case also has a smooth and decreasing pattern. It is worth noting that the terminal angle of attack is nonzero for all cases, which indicates the effect of omitted dynamics during derivation. Furthermore, when the initial ZEM is 0km, which indicates that no further course correction is required, the guidance law issued a zero angle of attack command and resulted in an identical trajectory to the ideal zero-effort case. This underscores the importance of including the reentry burn phase in the prediction. The extended partial-closed form solution can incorporate the reentry burn phase, thereby reducing unnecessary maneuvers. Lastly, the average computational time to predict descent trajectory was about 4.8 ms as in Fig. 4d, which shows promising performance in terms of onboard applications.

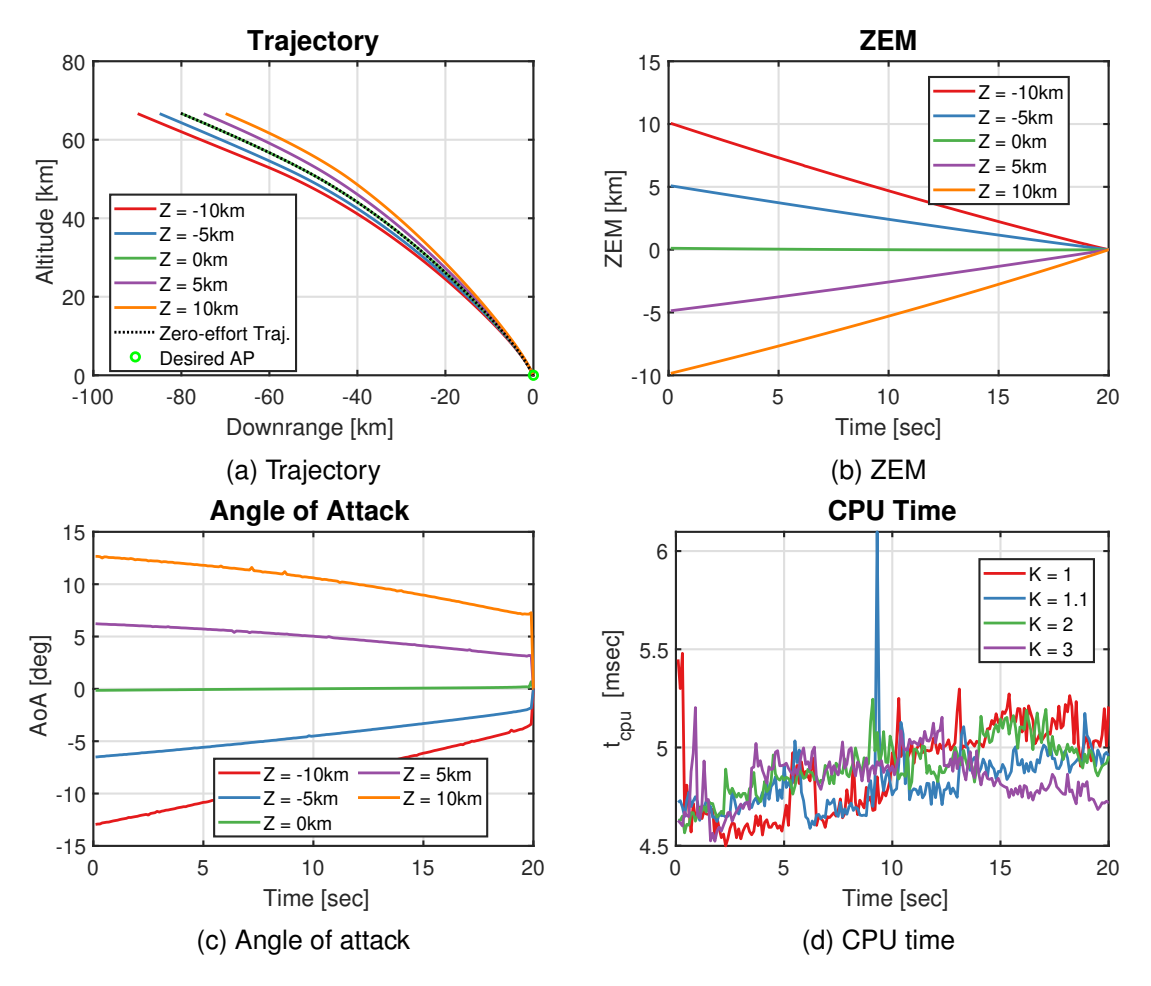


Figure 4 – Simulation results with various initial ZEMs.

4.2 Case Study - Guidance Gain

To investigate the guidance performance and convergence property, numerical simulation is conducted with varying guidance gain and the results can be seen in Fig. 5. First, for all cases with K from 1 to 3, the proposed guidance law successfully controlled RLV's downrange distance to the desired position. As investigated in Section 3, the proposed guidance possesses sub-optimality in preserving the ΔV during reentry burn, and the degree of the optimality depends on the weighting function in Fig. 5f. As the guidance gain increases from 1, W(t) shows skewed profile, degrading the optimality. This difference reveals itself in Figs. 5d and 5e, where the velocity difference and maximum dynamic pressure increase with increasing K. The reason velocity difference decreases during the reentry burn is mainly due to the flight path angle difference, which decreases velocity increase from gravitational attraction.

To verify the convergence analysis in the previous section, the case with K=1.1 is also conducted. Interestingly, both cases with K=1 and 1.1 have non-zero α at the end of the guidance. This implies that K=1.1 is not enough to meet the sufficient condition suggested in Eq. (28). Nevertheless, for the cases with K=2 and 3, the angle of attack converged to 0. This result partially verifies Condition 1 as the sufficient condition, which argues that a large enough gain K can guarantee $\alpha(t_f)=0$.

5. Conclusion

In this work, a simple feedback guidance law for reusable launch vehicles is proposed for down-range distance control for reusable launch vehicles (RLVs). The proposed law is based on the rapid trajectory prediction method that encompasses reentry burn and aerodynamic descent and utilizes finite-time convergent error dynamics. The theoretical analysis indicates the sub-optimality of the proposed method in preserving the desired ΔV during the reentry burn. Also, the proposed guidance law can have disturbance rejecting property and can guarantee the vehicle's angle of attack to

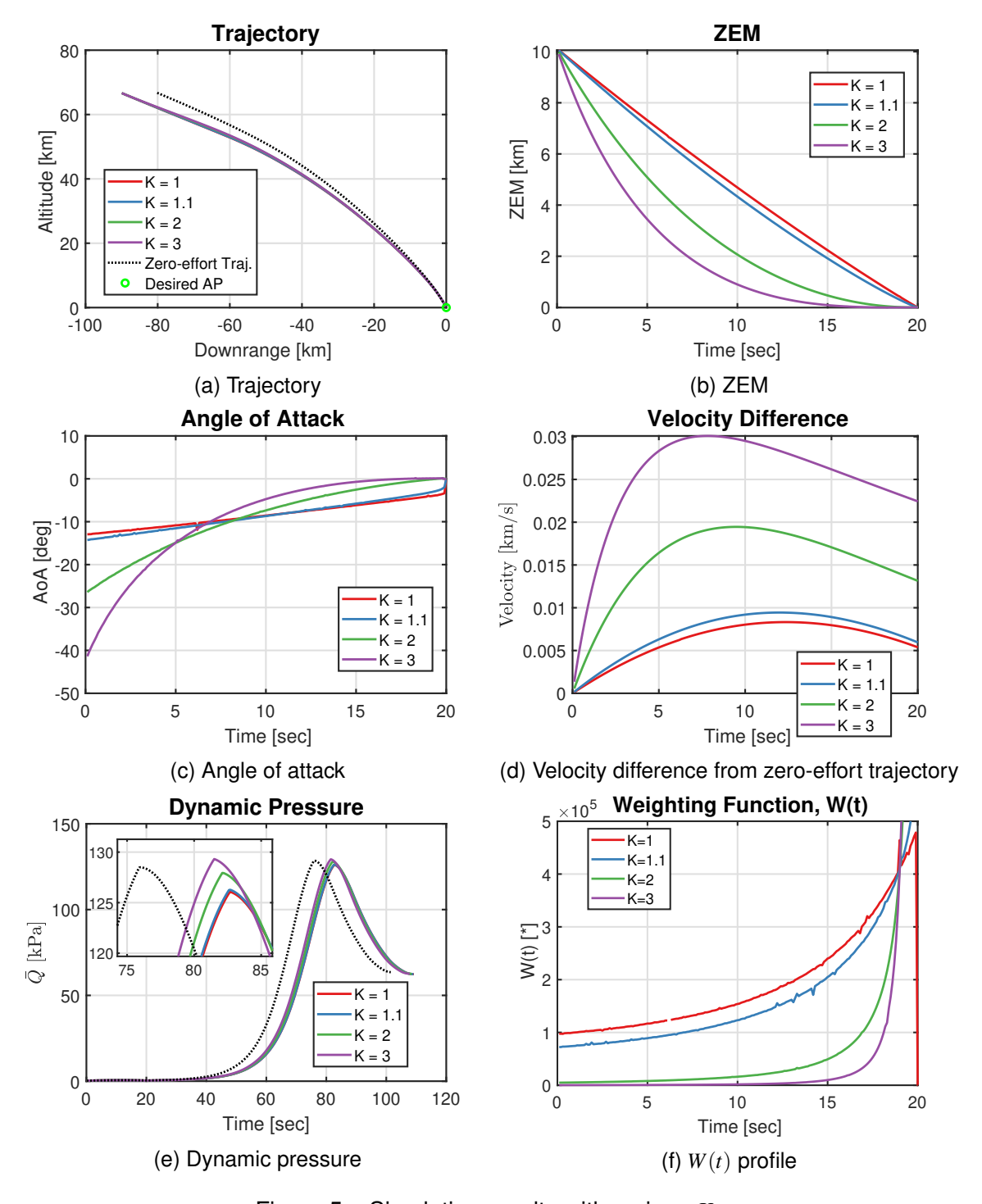


Figure 5 – Simulation results with various Ks.

become 0, which is beneficial to the preparation of the atmospheric reentry. The effectiveness and properties of the proposed method are verified by the numerical simulations with realistic parameters. The computational efficiency of the proposed rapid trajectory is also verified, which underscores the applicability of the proposed algorithm. In conclusion, the guidance law presented in this work can reduce the trajectory deviation of the RLV prior to reentry, ultimately supporting reliable operations of the RLVs.

6. Contact Author Email Address

Chang-Hun Lee (corresponding author): lckdgns@kaist.ac.kr

7. Copyright Statement

The authors confirm that they, and/or their company or organization, hold copyright on all of the original material included in this paper. The authors also confirm that they have obtained permission, from the copyright holder of any third party material included in this paper, to publish it as part of their paper. The authors confirm that they give permission, or have obtained permission from the copyright holder of this paper, for the publication and distribution of this paper as part of the ICAS proceedings or as individual off-prints from the proceedings.

8. Acknowledgment

This work was supported by the National Research Foundation of Korea (NRF) grant funded by the Korea government(MSIT) (No. NRF-2022M1A3B8065627).

References

- [1] Behçet Açikmeşe and Scott R. Ploen. Convex programming approach to powered descent guidance for mars landing. *Journal of Guidance, Control, and Dynamics*, 30(5):1353–1366, 2007.
- [2] Jaemyung Ahn and Woong Rae Roh. Noniterative instantaneous impact point prediction algorithm for launch operations. *Journal of Guidance, Control, and Dynamics*, 35(2):645–648, 2012.
- [3] Byeong-Un Jo and Jaemyung Ahn. Near time-optimal feedback instantaneous impact point (IIP) guidance law for rocket. *Aerospace Science and Technology*, 76:523–529, May 2018.
- [4] Byeong-Un Jo, Jaemyung Ahn, and Woong-Rae Roh. Instantaneous Impact Point Guidance Considering Uncertainty in Engine Cutoff Time. *Journal of Guidance, Control, and Dynamics*, 43(2):373–382, February 2020.
- [5] Ji Yeon An, Chang Hun Lee, and Min Jea Tahk. A Collision Geometry-Based Guidance Law for Course-Correction-Projectile. *International Journal of Aeronautical and Space Sciences*, 20(2):442–458, 2019. Publisher: The Korean Society for Aeronautical & Space Sciences (KSAS).
- [6] Ki-Wook Jung, Chang-Hun Lee, Junseong Lee, Sunghyuck Im, Keejoo Lee, Marco Sagliano, and David Seelbinder. An Instantaneous Impact Point Guidance for Rocket with Aerodynamics Control. In 2021 21st International Conference on Control, Automation and Systems (ICCAS), pages 1489–1495, Jeju, Korea, Republic of, October 2021. IEEE.
- [7] Peter Chudinov. Approximate Analytical Description of the Projectile Motion with a Quadratic Drag Force. *Athens Journal of Sciences*, 1(2):97–106, 2014.
- [8] Marco Sagliano, Ansgar Heidecker, José Macés Hernández, Stefano Farì, Markus Schlotterer, Svenja Woicke, David Seelbinder, and Etienne Dumont. Onboard Guidance for Reusable Rockets: Aerodynamic Descent and Powered Landing. In AIAA Scitech 2021 Forum, VIRTUAL EVENT, January 2021. American Institute of Aeronautics and Astronautics.
- [9] Shaoming He and Chang Hun Lee. Optimality of error dynamics in missile guidance problems. *Journal of Guidance, Control, and Dynamics*, 41(7):1620–1629, 2018.
- [10] Pedro Simplício, Andrés Marcos, and Samir Bennani. Reusable Launchers: Development of a Coupled Flight Mechanics, Guidance, and Control Benchmark. *Journal of Spacecraft and Rockets*, 57(1):74–89, 2020.